ChemComm

COMMUNICATION

View Article Online
View Journal | View Issue

Cite this: *Chem. Commun.*, 2016, 52, 6103

Received 29th January 2016,
Accepted 24th March 2016

DOI: 10.1039/c6cc00936k

www.rsc.org/chemcomm

Redox-active tetraruthenium metallacycles: reversible release of up to eight electrons resulting in strong electrochromism†

Daniel Fink, Bernhard Weibert and Rainer F. Winter*

Tetraruthenium macrocycles with 1,4-divinylphenylene and diarylamine-substituted isophthalic acids as the sides display up to eight one-electron redox steps and rich electrochromic behaviour with strong absorptions of the dications in the near infrared and of the tetra- and hexacations at low energies in the visible.

Metallacycles are typically constructed from metal coligand fragments as nodes and two kinds of ditopic bridging ligands, so-called linkers as the sides. The shapes and sizes of such structures are determined by the preferred coordination geometries of the metal ions and the topologies of the linkers. Hence, a great number of metallacycles with vastly different architectures and astounding levels of complexity have been realized.[1–6] Considering that many of these structures contain redox-active metal ions or linkers, or even both, only relatively few studies were specifically devoted to investigating or capitalizing on that property. Inherent perspectives such as triggering changes in guest-binding inside the cavities of metallacycles, manipulating their optical and magnetic properties, or studying intracage charge transfer phenomena have only sporadically been tackled. The elegant work of Hupp and coworkers, who explored charge transfer between diimine or porphyrinic linkers in mixed-valent tetrarhenium rectangles with ligand-based redox activity,[7–10] and of Kaim, Stang and Therrien on tetraplatinum, -rhenium or -ruthenium metallacycles with oxidizable or reducible linkers stand as instructive examples.[11–16]

We here report on tetraruthenium metallacycles which are constructed from two pairs of diruthenium 1,4-divinylphenylene- and triarylamine-derived ditopic linkers as two different kinds of redox-active entities that allow for the pairwise release of up to eight electrons per macrocycle resulting in strong polyelectrochromism.[17–19] Discrete divinylphenylene-bridged diruthenium complexes $\{Ru(CO)(L)(P^iPr_3)_2\}_2(\mu\text{-}CH{=}CH\text{–}C_6H_4\text{–}CH{=}CH\text{-}1,4)$ (L = mono- or bidentate monoanionic ligand) are generally oxidized in two consecutive, reversible one-electron steps. Their mixed-valent radical cations exhibit complete charge and spin delocalization as is indicated by the observation of just one Ru(CO) IR-band (the observed small band splitting arises from the non-degeneracy of the symmetrical and antisymmetrical Ru(CO) stretching vibrations) and resolved EPR hyperfine splitting of the unpaired spin to four equivalent ^{31}P nuclei of the P^iPr_3 coligands.[20,21] Triarylamines constitute paradigmatic organic redox-systems and have found great use as selective oxidants and in redox catalysis.[22–26] More electron-rich representatives can be further oxidized to persistent dications.[26] A macrocycle constructed from two of these entities each may thus reversibly release six or even eight electrons per macrocycle.[27,28]

When the 1,4-divinylphenylene-bridged diruthenium complex **1-Cl** as 180° building block was combined with diphenyl- or (di-4-anisylamino)benzene-3,5-dicarboxylic acid (**2-H** or **2-OMe**) as a 0° building block[4] with K_2CO_3 base in $MeOH/CH_2Cl$ 1 : 1, a complex mixture of products was initially formed as indicated by the presence of several sets of vinyl proton and ^{31}P NMR signals.

On further warming to 50 °C for 48 h that mixture became uniform, showing just one set of proton NMR signals for the divinylphenylene and dicarboxylate building blocks and a single ^{31}P NMR resonance. Target macrocycles **3-H** and **3-OMe** (Scheme 1) were isolated in yields of *ca.* 60% as pale yellow microcrystalline solids and were characterized by ^1H, $^{13}C\{^1H\}$ and $^{31}P\{^1H\}$ NMR spectroscopy, ESI-MS and combustion analysis (ESI†).

Crystals of **3-OMe** that lent themselves for X-ray crystallography were grown from benzene/MeOH and CH_2Cl_2/MeOH, respectively, and the results are shown in Fig. 1. In both structures, the divinylphenylene diruthenium moieties adopt a *cisoid* conformation and both vinyl groups point outward the inner cavity of the metallamacrocycle. This generates an oval cavity of approximate dimensions of 7.9 Å × 12.4 Å or 7.8 Å × 12.4 Å as measured between opposing hydrogen atoms. Forcing the divinylphenylene units into a metallamacrocyclic ring causes some minor torsional strain. In the benzene solvate **3-OMe**·$7C_6H_6$ this strain is evident from the torsion

Fachbereich Chemie, Universität Konstanz, Universitätsstraße 10, D-78453 Konstanz, Germany. E-mail: rainer.winter@uni-konstanz.de

† Electronic supplementary information (ESI) available: Experimental procedures, characterization, NMR and mass spectra, X-ray crystallography, voltammograms, spectroelectrochemistry. CCDC 1450420 and 1450421. For ESI and crystallographic data in CIF or other electronic format see DOI: 10.1039/c6cc00936k

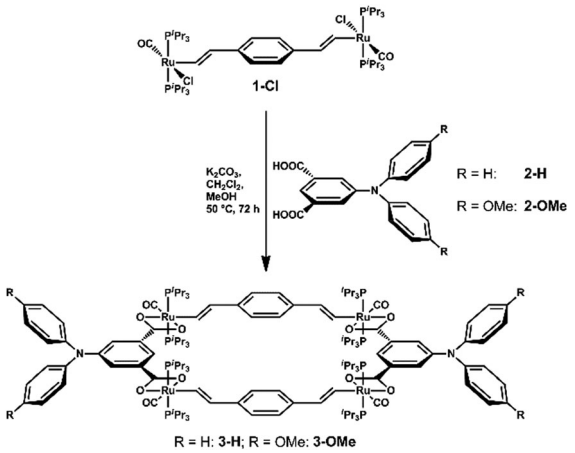

Scheme 1 Synthesis of the tetraruthenium metallamacrocycles.

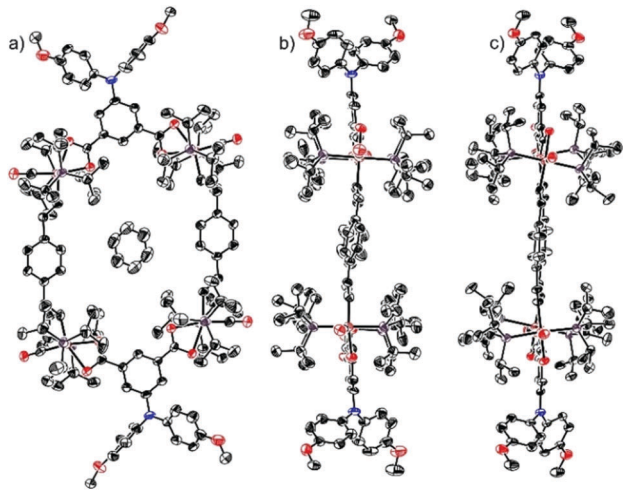

Fig. 1 Structures of **3-OMe** as the benzene solvate (a) top view, (b) side view and (c) side view of the CH_2Cl_2 solvate. Solvent molecules other than the benzene molecule in the cavity and hydrogen atoms are removed for reasons of clarity. The ellipsoids are displayed at a 50% probability level.

of one ruthenium alkenyl moiety of each divinylphenylene linker by ϕ = 27.3° with respect to the adjacent phenylene ring whereas the other remains in a more coplanar arrangement with ϕ = 6.6°. Torsional angles O–C–C–C at the benzene-3,5-dicarboxylates of 7.6 and 4.5° and at the Ru–C═C–C linkages of 3.5 and 4.8° are nearly ideal and the P–Ru–P vectors of opposing nodes are almost parallel as indicated by P–Ru–Ru–P torsion angles of 3.5 and 4.1°. In the dichloromethane solvate **3-OMe**·$8CH_2Cl_2$ the divinylphenylene moieties achieve a somewhat higher degree of coplanarity with the central phenylene rings with torsion angles ϕ of 10.8 and 13.3° while the torsional angles O–C–C–C and Ru–C═C–C are larger at 7.2° and 14.9° or 7.2° and 8.4°. The overall result is a twist of the P–Ru–P vectors as measured by P–Ru–Ru–P torsions of 19.0° and 21.9°, which in turn induces a bending of one divinylphenylene moiety to above and the other one to below the mean plane of the macrocycle (Fig. 1c). The two structures can thus be viewed as snapshots demonstrating the conformational degrees of freedom inherent to these macrocycles.

In **3-OMe**·$7C_6H_6$, one molecule of benzene stacks in a coplanar, but laterally offset fashion with respect to the divinylphenylene sides, whereas the cavity of the CH_2Cl_2 solvate accommodates two solvent molecules that show no H-bonding interactions or short contacts with the cavity walls (see ESI†). This indicates that the tetraruthenium macrocycles, like other structures of this type, might also exhibit interesting host–guest chemistry.[29,30]

The electrochemical properties of macrocycles **3-H** and **3-OMe** are best compared to those of precursor **1-Cl** and its bis(benzoato) substitution product, {Ru(CO)(P^iPr_3)$_2$(κ^2*O*,*O*′-OOCPh)}$_2$(μ-CH═CH–C_6H_4–CH═CH-1,4) (**1-OOCPh**). Both complexes display two consecutive, reversible one-electron waves at half-wave potentials $E_{1/2}$ of −0.09 and +0.17 V[20] or −0.25 and +0.02 V, respectively.[31] The cathodic shift of ∼150 mV on substitution of the chloro by the benzoato ligands follows the increase in valence electron count at the Ru atoms from 16 to 18 and the concomitant raise in energy of the redox-orbital(s), which receive major contributions from the π-conjugated bridging ligand.[20,21,32–37] For **3-H**, three consecutive waves are apparent in the cyclic voltammograms (CH_2Cl_2/NBu_4PF_6, Fig. 2). On close inspection one notes a small splitting of the first wave into two closely spaced one-electron processes. No such effect is however seen for the second and third waves. $E_{1/2}$ values under these conditions are summarized in Table 1. Nearly identical results were obtained with the even less ion-pairing B{$C_6H_3(CF_3)_2$-3,5}$_4^-$ counterion (ESI†). Since all waves are associated with similar peak currents and based on the overall composition and potentials we can safely assign the first two composite waves as the oxidations of the divinylphenylene sides and the

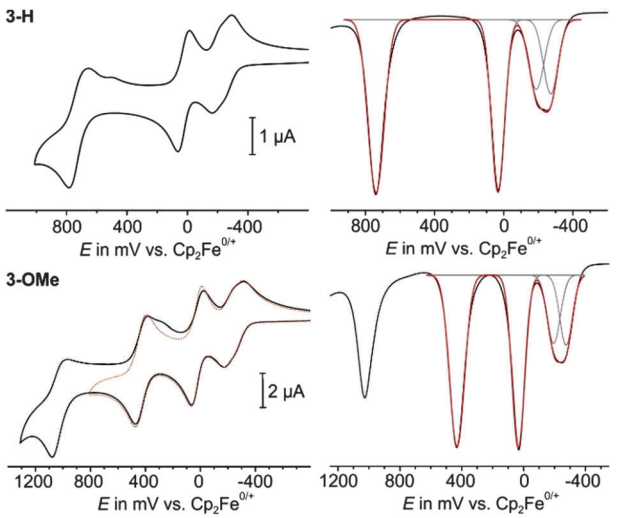

Fig. 2 Cyclic voltammograms (CH_2Cl_2/0.1 M NBu_4PF_6, r.t. at v = 0.1 V s^{-1}) (left) and square wave voltammograms (right) of **3-H** and **3-OMe** along with deconvolutions.

Table 1 Half-wave potentials of metallamacrocycles **3-H** and **3-OMe** in mV *vs.* $Cp_2Fe^{0/+}$

	$E_{1/2}^{0/+}$	$E_{1/2}^{+/2+}$	$E_{1/2}^{2+/4+}$	$E_{1/2}^{4+/6+}$	$E_{1/2}^{6+/8+}$
3-H	−272	−188	33	739	—
3-OMe	−275	−194	34	431	1026

third wave as the concurrent oxidations of the amine appendices. Thus, all three waves correspond to two closely spaced or coincident one-electron processes.

In the case of **3-OMe**, a fourth such wave is seen close to the anodic discharge limit of the electrolyte, which obviously corresponds to the second oxidations of the peripheral triarylamine sites (Fig. 2). The above assignments are reconfirmed by the fact that substitution of the phenyl by anisyl substituents only affects the redox potentials past the 4+ states (Table 1).

Bis(alkenylarylene)-bridged diruthenium complexes with extended conjugated bridging ligands and [2.2]paracyclophanyl-bridged analogs with cofacial and coplanar arranged styryl decks were found to exhibit rather substantial degrees of ground-state delocalization in the mixed-valent states despite potential splittings $\Delta E_{1/2}$ near the purely statistical limit.[32,38] This is, however, not the case here as shown by the results of IR and UV/Vis/NIR (NIR = near infrared) spectroelectrochemistry. Spectroscopic changes on the first composite two-electron oxidation, where one electron is removed from each divinylphenylene diruthenium entity, are essentially identical to the first oxidation of **1-Cl** or **1-OOCPh**. Thus, the Ru(CO) IR band blue-shifts by 34 cm^{-1} with some discernible splitting into a less intense band at higher and a more intense one at lower energy (Fig. 3 and ESI†). That splitting is due to a non-degeneracy of the symmetrical and antisymmetrical combinations of Ru(CO) stretches. Further spectroscopic changes include the growth of bands in the region of ring stretching and bending vibrations and of an intense absorption in the NIR at *ca.* 7700 cm^{-1} (ESI†). That band also shows up as part of an intense, structured NIR absorption in the UV/Vis/NIR experiments along with an equally intense one in the Vis (see Table 2, Fig. 3 and ESI†). Characteristic spectroscopic data are collected in Table 2.

The relation between $\Delta E_{1/2}$ (in Volts) and K_c, the equilibrium constant of the comproportionation reaction **3-H**$^{2+}$ + **3-H** ⇄ 2 **3-H**$^{+}$, $K_c = \exp[n{\cdot}F{\cdot}\Delta E_{1/2}/(R{\cdot}T)] = \exp(39.33{\cdot}\Delta E_{1/2})$ at T = 295 K dictates that, after release of one equivalent of charge, the mixed-valent (MV) forms **3-H**$^{+}$ or **3-OMe**$^{+}$ are the dominant species in the equilibrated solutions, even when $\Delta E_{1/2}$ is vanishingly small. Still, no spectrum recorded during electrolysis has features other than those corresponding to the respective dications and the neutral precursors and, in particular, none that could be ascribed to charge transfer from the remaining reduced divinylphenylene side to the already oxidized one. This means that the radical cations are mixed-valent species of Class I with non-interacting redox sites.[39,40] Obviously the dicarboxylic linkers, which do not contribute to the redox orbitals HOMO and HOMO−1,[31,41] and the lateral positioning of the divinylphenylene moieties of the macrocycles mutually insulate the two divinylphenylene sides from each other. As a consequence, **3-H**$^{2+}$ and **3-OMe**$^{2+}$ are EPR active and display a somewhat broad isotropic signal at g = 2.039 (ESI†).

The same overall behaviour repeats on the second composite oxidation encompassing the concurrent 2+/3+ and the 3+/4+ waves, corresponding to the second oxidation of the divinylphenylene sides (Fig. 3 and ESI†). Thus, the overall spectroscopic changes with a further blue-shift of the Ru(CO) band by *ca.* 40 cm^{-1}, the collapse of the NIR band and the further growth

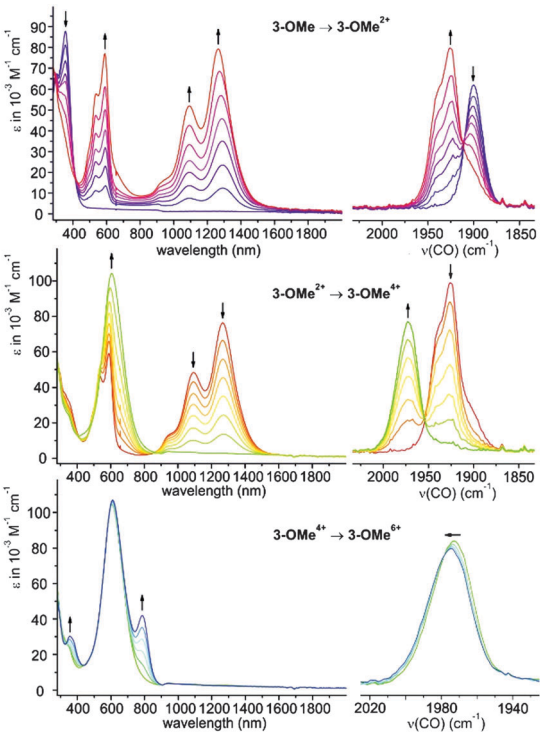

Fig. 3 Changes in the UV/Vis/NIR (left) and in the ν(CO) region of the IR spectra (right) of macrocyle **3-OMe** upon oxidation to **3-OMe**$^{2+}$ (top), **3-OMe**$^{4+}$ (middle) and **3-OMe**$^{6+}$ (bottom) (CH_2Cl_2/NBu_4PF_6, r.t.).

Table 2 Characteristic spectroscopic data for macrocycles **3-H** and **3-OMe** in all their accessible oxidation states

	ν(CO) (cm^{-1})	λ (nm) ($\varepsilon \times 10^{-3}$ (M^{-1} cm^{-1}))
3-H	1901	306 (60.3), 357 (75.6)
3-H^{2+}	1943, 1927	293 (49.8), 538 (42.4), 590 (60.4), 1093 (36.0), 1267 (59.9)
3-H^{4+}	1975	276 (53.1), 605 (101.9)
3-OMe	1900	304 (67.4), 355 (87.8)
3-OMe^{2+}	1942, 1925	282 (70.3), 537 (57.8), 590 (76.9), 1093 (52.0), 1267 (79.4)
3-OMe^{4+}	1973	276 (60.2), 606 (104.3)
3-OMe^{6+}	1975	275 (54.5), 354 (30.4), 610 (107.0), 787 (42.1)

of the Vis absorption are very similar or virtually identical to those observed on the second oxidation of diruthenium complexes **1-Cl** and **1-OOCPh**. Again, no absorption bands other than those of the di- and tetracations are seen at intermediate stages of the electrolysis where **3-H**$^{3+}$ or **3-OMe**$^{3+}$ constitute the major species in solution. Hence, the trications are also valence localized MV species of Class I. The divinylphenylene diruthenium entities thus behave as two independent electrophoric units and the only consequence of forging two of them together in a metallacyclic structure is a predictable doubling of molar extinction coefficients to rather impressive values of *ca.* 80 000 for the prominent NIR absorption of **3-OMe**$^{2+}$ and >100 000 for the Vis band of **3-OMe**$^{4+}$ (neutral **3-OMe** is transparent in these regimes).

Owing to the inherent instability of **3-H**$^{6+}$, the spectral consequences of further oxidizing the triarylamine appendices

could only be monitored for **3-OMe**. They include a very modest shift of the Ru(CO) IR band from 1973 to 1975 cm^{-1} and of the prominent Vis band from 606 nm in **3-OMe**$^{4+}$ to 610 nm in **3-OMe**$^{6+}$ (see Table 2). Additional bands at 354 nm and at 787 nm with extinction coefficients of 30 400 and 42 100 M^{-1} cm^{-1} closely resemble those of the radical cation of **2-OMe** (λ_{max} = 365, 793 nm).[42] Moreover, chemically generated **3-OMe**$^{6+}$ displays a non-binomial triplet at g = 2.014 and a ^{14}N hyperfine splitting of 9.6 G in its EPR spectrum as it is typical of aminium-type radicals,[43] thereby reconfirming the above assignments of the individual redox processes (ESI†). The only negligible impact of amine oxidation on the position of the $\pi \rightarrow \pi^*$ absorption band of the bis(oxidized) divinylphenylene diruthenium entities and the Ru(CO) band shifts further emphasizes the lack of electronic interaction between the two different kinds of redox sites. Further oxidation to **3-OMe**$^{8+}$ was, however, not possible under the conditions of spectroelectrochemistry, probably due to the proximity of that wave to the solvent background and a poor solubility of this polycation.

In conclusion, we have prepared and investigated amine-functionalized tetraruthenium metallamacrocycles in good yields from divinylphenylene–diruthenium complexes and amine functionalized isophthalic acids. These compounds can be oxidized by up to eight electrons with stepwise charge loss from the divinylphenylene linkers and the triarylamine appendices. Spectroscopic consequences of oxidation up to **3-OMe**$^{6+}$ were monitored by IR and UV/Vis/NIR spectroelectrochemistry and revealed strongly electrochromic behaviour.[44] The lateral placement of the redox-active divinylphenylene entities and the insulating nature of the dicarboxylate linkers shut down intramolecular charge transfer between the individual redox sites and lead to paramagnetic behaviour.

The authors thank Maximilian Dürr and Ivana Ivanović-Burmazović from the Friedrich-Alexander Universität Erlangen-Nürnberg for the acquisition of the ESI-MS spectra and Stefan Scheerer for the recording and simulation of the EPR spectra.

Notes and references

1 M. Fujita, M. Tominaga, A. Hori and B. Therrien, *Acc. Chem. Res.*, 2005, **38**, 369–378.
2 C. G. Oliveri, P. A. Ulmann, M. J. Wiester and C. A. Mirkin, *Acc. Chem. Res.*, 2008, **41**, 1618–1629.
3 Y.-F. Han, W.-G. Jia, W.-B. Yu and G.-X. Jin, *Chem. Soc. Rev.*, 2009, **38**, 3419–3434.
4 R. Chakrabarty, P. S. Mukherjee and P. J. Stang, *Chem. Rev.*, 2011, **111**, 6810–6918.
5 M. M. J. Smulders, I. A. Riddell, C. Browne and J. R. Nitschke, *Chem. Soc. Rev.*, 2013, **42**, 1728–1754.
6 M. Han, D. M. Engelhard and G. H. Clever, *Chem. Soc. Rev.*, 2014, **43**, 1848–1860.
7 P. H. Dinolfo, M. E. Williams, C. L. Stern and J. T. Hupp, *J. Am. Chem. Soc.*, 2004, **126**, 12989–13001.
8 P. H. Dinolfo and J. T. Hupp, *J. Am. Chem. Soc.*, 2004, **126**, 16814–16819.
9 P. H. Dinolfo, S. J. Lee, V. Coropceanu, J.-L. Brédas and J. T. Hupp, *Inorg. Chem.*, 2005, **44**, 5789–5797.
10 P. H. Dinolfo, V. Coropceanu, J.-L. Brédas and J. T. Hupp, *J. Am. Chem. Soc.*, 2006, **128**, 12592–12593.
11 H. Hartmann, S. Berger, R. Winter, J. Fiedler and W. Kaim, *Inorg. Chem.*, 2000, **39**, 4977–4980.
12 W. Kaim, B. Schwederski, A. Dogan, J. Fiedler, C. J. Kuehl and P. J. Stang, *Inorg. Chem.*, 2002, **41**, 4025–4028.
13 N. Das, A. M. Arif, P. J. Stang, M. Sieger, B. Sarkar, W. Kaim and J. Fiedler, *Inorg. Chem.*, 2005, **44**, 5798–5804.
14 J. Mattsson, P. Govindaswamy, A. K. Renfrew, P. J. Dyson, P. Štěpnička, G. Süss-Fink and B. Therrien, *Organometallics*, 2009, **28**, 4350–4357.
15 V. Vajpayee, S. Bivaud, S. Goeb, V. Croué, M. Allain, B. V. Popp, A. Garci, B. Therrien and M. Sallé, *Organometallics*, 2014, **33**, 1651–1658.
16 M. Yuan, F. Weisser, B. Sarkar, A. Garci, P. Braunstein, L. Routaboul and B. Therrien, *Organometallics*, 2014, **33**, 5043–5045.
17 R. J. Mortimer, *Chem. Soc. Rev.*, 1997, **26**, 147–156.
18 M. D. Ward, *J. Solid State Electrochem.*, 2005, **9**, 778–787.
19 R. J. Mortimer, *Annu. Rev. Mater. Res.*, 2011, **41**, 241–268.
20 J. Maurer, B. Sarkar, B. Schwederski, W. Kaim, R. F. Winter and S. Záliš, *Organometallics*, 2006, **25**, 3701–3712.
21 S. Záliš, R. F. Winter and W. Kaim, *Coord. Chem. Rev.*, 2010, **254**, 1383–1396.
22 E. Steckhan, *Angew. Chem., Int. Ed. Engl.*, 1986, **25**, 683–701.
23 S. Dapperheld, E. Steckhan, K.-H. G. Brinkhaus and T. Esch, *Chem. Ber.*, 1991, **124**, 2557–2567.
24 N. G. Connelly and W. E. Geiger, *Chem. Rev.*, 1996, **96**, 877–910.
25 T. P. Bender, J. F. Graham and J. M. Duff, *Chem. Mater.*, 2001, **13**, 4105–4111.
26 S. Amthor, B. Noller and C. Lambert, *Chem. Phys.*, 2005, **316**, 141–152.
27 C.-Y. Yao, J. Yao and Y.-W. Zhong, *Inorg. Chem.*, 2011, **50**, 6847–6849.
28 J.-H. Tang, S.-H. Wu, J.-Y. Shao, H.-J. Nie and Y.-W. Zhong, *Organometallics*, 2013, **32**, 4564–4570.
29 B. Therrien, *Eur. J. Inorg. Chem.*, 2009, 2445–2453.
30 N. P. E. Barry, O. Zava, P. J. Dyson and B. Therrien, *J. Organomet. Chem.*, 2012, **705**, 1–6.
31 E. Wuttke, Y.-M. Hervault, W. Polit, M. Linseis, P. Erler, S. Rigaut and R. F. Winter, *Organometallics*, 2014, **33**, 4672–4686.
32 M. Linseis, S. Záliš, M. Zabel and R. F. Winter, *J. Am. Chem. Soc.*, 2012, **134**, 16671–16692.
33 P. Mücke, M. Linseis, S. Záliš and R. F. Winter, *Inorg. Chim. Acta*, 2011, **374**, 36–50.
34 W. Y. Man, J.-L. Xia, N. J. Brown, J. D. Farmer, D. S. Yufit, J. A. K. Howard, S. H. Liu and P. J. Low, *Organometallics*, 2011, **30**, 1852–1858.
35 U. Pfaff, A. Hildebrandt, M. Korb, S. Oßwald, M. Linseis, K. Schreiter, S. Spange, R. F. Winter and H. Lang, *Chem. – Eur. J.*, 2016, **22**, 783–801.
36 S. Scheerer, N. Rotthowe, O. S. Abdel-Rahman, X. He, S. Rigaut, H. Kvapilová, S. Záliš and R. F. Winter, *Inorg. Chem.*, 2015, **54**, 3387–3402.
37 Y.-P. Ou, J. Zhang, M. Xu, J. Xia, F. Hartl, J. Yin, G.-A. Yu and S. H. Liu, *Chem. – Asian J.*, 2014, **9**, 1152–1160.
38 P. Mücke, M. Zabel, R. Edge, D. Collison, S. Clément, S. Záliš and R. F. Winter, *J. Organomet. Chem.*, 2011, **696**, 3186–3197.
39 M. B. Robin and P. Day, *Adv. Inorg. Chem. Radiochem.*, 1967, **10**, 247–422.
40 B. Brunschwig, C. Creutz and N. Sutin, *Chem. Soc. Rev.*, 2002, **31**, 168–184.
41 F. Pevny, R. F. Winter, B. Sarkar and S. Záliš, *Dalton Trans.*, 2010, 8000–8011.
42 H. Murata and P. M. Lahti, *J. Org. Chem.*, 2007, **72**, 4974–4977.
43 G. A. Pearson, M. Rocek and R. I. Walter, *J. Phys. Chem.*, 1978, **82**, 1185–1192.
44 N. Deibel, M. G. Sommer, S. Hohloch, J. Schwann, D. Schweinfurth, F. Ehret and B. Sarkar, *Organometallics*, 2014, **33**, 4756–4765.

